Biochimica et Biophysica Acta, 1104 (1992) 233–242

BBAMEM 75543

The sodium channel activator Brevetoxin-3 uncovers a multiplicity of different open states of the cardiac sodium channel

Wolfgang Schreibmayer and Gerhard Jeglitsch

Institute of Medical Physics and Biophysics, Karl-Franzens-University Graz, Graz (Austria)

(Received 1 October 1991)

Key words: Sodium ion channel; Brevetoxin; Patch clamp; (Heart); (Rat ventricular myocyte)

The interaction of Brevetoxin 3 (Pbtx-3), a sodium channel activator, with the cardiac sodium channel was studied at the single channel level. It was found that Pbtx-3 (20 μM) shifted steady-state activation to negative potentials, without major effects on the time course of macroscopic activation or macroscopic currents decay, as calculated from averaged single-channel records. Single-channel open times were found to be prolonged. Under the influence of the toxin, sodium channel openings could be observed frequently even at maintained depolarisation. These openings occurred to at least nine different subconductance levels of the open state with smaller conductivities than the maximal one and differed in their open times. Current amplitudes of these open substates were found to cluster around certain amplitude values. Appearance of substates at maintained depolarisation was dependent on the transmembrane potential (E_m): Substates with smaller conductivity appeared more frequently at lower E_m values whereas at higher E_m values substates with higher conductivity values dominated. Furthermore, it was demonstrated that appearance of substates did not result from incomplete recovery from inactivation. From these observations it was concluded that the open substates observed correspond to different conformational states of the channel's activation gates. Under physiological conditions, when the sodium channel opens directly from its closed state these 'incomplete'-open states of the cardiac sodium channel are obscured by fast gating transitions between the corresponding, electrically silent, preopen states. Thus, Pbtx-3 acts mainly via stabilisation of the channel's preopen and different open states. A classification of sodium channel modifiers, based on their interaction with different conformational states of the channel is suggested.

Introduction

Substates of open sodium channels, i.e. open states with conductivities smaller than the maximal possible one, were described initially for sodium channels modified by certain agents acting on the binding domain for plant alkaloids (Quandt and Narahashi [1] and Sigel [2]). Numerous substates of voltage-dependent sodium channels have been systematically described for the major isoforms of this channel, i.e. the neuronal (Nagy [3]), the skeletal (Patlak [4]) and the cardiac type (Schreibmayer et al. [5]). It has not been possible so far to assign any functional role to these substates, nor to give an explanation as to how these open substates might be linked to the conformational changes occurring during the normal gating process.

Therefore, studies with different sodium channel gating modifiers were undertaken in order to enhance certain conformational states of the cardiac sodium channel, i.e. to make these states accessible to exploration in greater detail. The interaction of Pbtx-3 with the cardiac sodium channel is described in this paper. Brevetoxins are cyclic polyethers, produced by marine dinoflagellates (Baden [6]) with neurotoxic properties on voltage-dependent sodium channels from nerve, cardiac and skeletal muscle (Borison et al. [7]). It has been shown by radioligand binding assays, that they occupy a separate binding-domain on the sodium channel protein (Lombet et al. [8] and Sharkey et al. [9]), that is distinct from those for (i) TTX, STX and Geographutoxin, (ii) plant alkaloids like veratridine, germitrine etc., (iii) anemone toxins and α-scorpion toxin, (iv) β-scorpion toxins and (v) pumiliotoxins (Gusovsky et al. [10]). Pbtx-3 turned out to be extremely useful in inducing open substates of the cardiac sodium channel that could be investigated in great detail and their voltage dependence studied.

Correspondence: W. Schreibmayer, Institute of Medical Physics and Biophysics, Karl-Franzens-University Graz, A-8010 Graz, Austria.

Materials and Methods

Cell preparation

Cardiac ventricular cells from adult rats were prepared essentially as described earlier (Schreibmayer et al. [11] and Schreibmayer et al. [12]). They were kept in culture for 4 h to 76 h after disaggregation. Before the electrophysiological experiments were started, cells were transferred to a petri-dish that was placed in a holder thermostated by a peltier-element to keep the temperature constant at 18°C. The cells were allowed to settle down and adhere to the bottom of the dish. Then excessive superfusion was performed to wash out remaining culture medium before the experiment was started. Micromanipulations (MO-103, Narishige, Japan; patch-clamp tower, List Medical Instruments, Germany) were performed under the visual control of an inverted microscope (Zeiss IM 35, Germany).

Single-channel recordings

Single-channel currents were recorded according to Hamill et al. [13] in the cell-attached configuration at 18°C. The membrane potential of the cardiac cells was set to zero by using a high concentration of external K^+. Pipets (American Glass Co.; glass type 7740, square id.) were pulled (L/M-3P-A puller; List Medical Instruments, Germany) to give resistance values between 5 and 20 MΩ, when filled with the pipet solution described below. Patch currents were amplified (Axopatch 3D with IHS integrating headstage; Axon Instruments, USA), filtered at 5 kHz (4-pole Bessel) and stored on PCM tape (Instrutech PCM processor, USA; in connection with a commercially available VTR). For voltage-clamp experiments voltage jumps were generated at variable frequencies stated in the figures and patch currents were directly digitized by an IBM compatible computer (Steiner 386; Austria) equipped with an A/D and D/A board (TL-125; Axon Instruments, USA), controlled by the Pclamp 5.03 software (Axon Instruments; USA).

Variance analysis

Patlak (1988) developed an algorithm for assessment of subconductance current levels based on their variance. We adopted this method for our purpose. The initial analysis developed by Patlak [4] used a fixed window along the time axis (this window included a defined number of adjacent current sample data points, n). The variance (σ^2) of the mean current within this window is calculated. By comparision of this σ^2 with a preset upper limit for σ^2, σ^2_{max}, the corresponding data point (the current sample in the middle of this window) is included into or rejected from analysis of channel current amplitude (I_c).

Thus, by using a fixed window size, data samples that do not belong, but are in the near vicinity of nonconducting-conducting state transitions are lost, leading to an overproportional exclusion of short states from amplitude analysis. To improve this situation a flexible window algorithm was developed by us (Schreibmayer and Russ, unpublished data): each current sample data point i that fulfilled the criteria to (i) belong to a continuous series of at least j data points with a calculated $\sigma_j^2 < \sigma^2_{max}$ and (ii) with a calculated individual deviation from the mean current calculated in this series $< \sigma_{max}$ (maximal standard deviation) was taken for subsequent analysis of I_c.

Recording solutions

The extracellular solution was hyperosmolar for preshrinking of the cardiomyocytes, contained high K^+ (in order to be able to use high [Na^+] in the pipette), and had the following composition (in mM): 218 KCl, 2.5 EGTA, 0.5 $MgCl_2$, 0.25 $CaCl_2$, 10 glucose and 10 Hepes. The solution was titrated with KOH to give a final pH of 7.2.

The pipet solution contained high Na^+ in order to improve resolution of sodium channel currents and contained (in mM): 300 NaCl, 5.4 KCl, 1.5 $CaCl_2$, 1.5 $MgCl_2$, 1 $BaCl_2$, 10 glucose and 10 Hepes and was titrated with NaOH to give a final pH value of 7.2.

Chemicals

HPLC purified PbTx-3 was kindly provided by D. Baden (Rosenstiel School of Marine and Atmospheric Science, Miami, USA)). Collagenase for cell disaggregation was purchased from Worthington (Type CI-28). All other reagents used were of analytical grade.

Results

Activation-inactivation kinetics of Pbtx-3-modified sodium channels

In order to elucitate sodium channel openings, depolarising voltage jumps were applied to cell-attached membrane patches, starting from a holding potential of -120 mV. When 20 μM Pbtx-3 was present in the patch pipette, the following effects of Pbtx-3 on sodium channel gating could be observed:

(i) Activation of single sodium channels could be observed at rather negative membrane potentials (E_m) compared to unmodified channels (cf. Figs. 1a and 1b). When open probabilities ($P_{(o)}$'s) were calculated from many single-channel records, it became obvious that $P_{(o)}$ for Pbtx-3-modified channels at e.g. -70 mV was considerably elevated, whereas it was close to zero at the same potential when no Pbtx-3 was present in the pipette (Figs. 1e and 1f). In order to quantitatively evaluate this obvious shift in steady state activation, normalized average peak inward currents (I_p's) were

measured for different E_m values. The resulting graph for controls and Pbtx-3 treated sodium channels is shown in Fig. 1i.

(ii) At more positive E_m values e.g. −40 mV the time course of sodium channel activation and inactivation was almost identical (see Figs. 1g and 1h for examples and 1j for evaluation at different potentials for controls and Pbtx-3). This indicates that steady-state sodium channel openings, induced by Pbtx-3 (see below), contribute only to a minor extent to the initial sodium inward current.

(iii) Single-channel open time seemed to be slightly prolonged at more positive E_m values (Figs. 1c and 1d), especially at −40 mV (see Fig. 1k).

(iv) Whereas rarely observed under control conditions, sublevel gating, i.e. single-channel openings with current amplitudes smaller than the maximal possible one, occurred frequently in membrane patches treated with 20 μM Pbtx-3 (marked with open circles in Fig. 1a).

(v) At control conditions sodium channel inactivation after onset of a depolarising step in E_m was

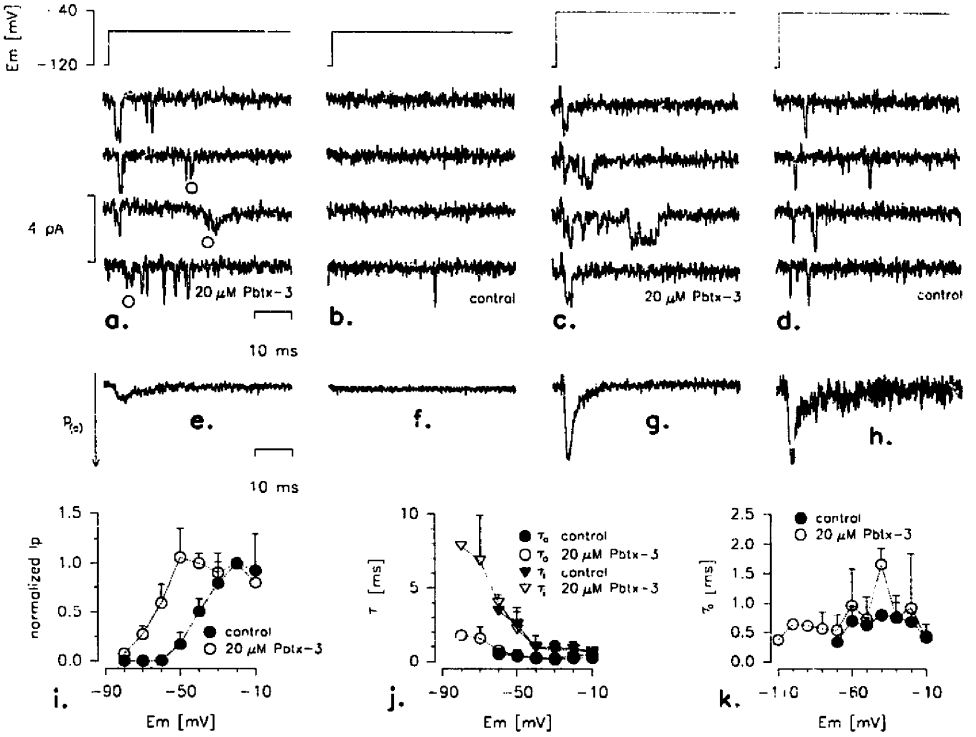

Fig. 1. Kinetics of Pbtx-3 modified and unmodified sodium channels after voltage jumps. (a) Sodium channel currents, modified by 20 μM Pbtx-3, were elicited in a cell-attached membrane patch by stepping E_m from −120 mV to −70 mV every 2 s for 50 ms (voltage jump protocol on top of panel a). Resulting patch currents were low pass filtered with a 4-pole Bessel filter at 5 kHz and digitized at a sample frequency of 33.3 kHz. The resulting records were digitally filtered at 3 kHz with a Gaussian filter algorithm. Records that did not contain sodium channel openings were averaged, and this average was subtracted from every individual record for digital compensation of the residual capacitance transient. The resulting records were stored for subsequent analysis; four representative records are displayed on panel a. Open channel substates are set out through open circles. (b, c and d) Same as (a), but controls at −70 mV (b), 20 μM Pbtx-3 at −40 mV (c) and controls at −40 mV (d). (e) Average current $P_{(o)}$ (downward deflection of the graph means increase in $P_{(o)}$), derived by averaging 80 consecutive records as shown in panel a but filtered digitally at 1.5 kHz. (f, g and h) Same as (e), but (f), (g) and (h) corresponding to (b), (c) and (d), respectively. (i) Normalized average peak inward current (I_p) vs. E_m. I_p values were directly measured from averaged single channel records such as shown in (e–h). In order to account for the variability in the number of active channels in a given patch, I_e values were normalized to the I_p measured at −20 mV for a given patch. Filled circles (●): mean I_p values ± standard deviations (S.D.) for controls ($n = 4$). Open circles (○): mean I_p values ± S.D. at 20 μM Pbtx-3 ($n = 4$). (j) Time constants for activation and inactivation of averaged single-channel records. Simple exponential functions were fitted into the rising and decaying phases of $P_{(o)}$ vs. time (digital filtering at 1.5 kHz). Mean values ± S.D. derived from four different membrane patches each for controls and 20 μM Pbtx-3, respectively, are shown. (k) Open times of control sodium channels and those modified with 20 μM Pbtx-3 after onset of the voltage jump. Single-channel records were digitally filtered at 1.5 kHz and individual open times measured. The open time distributions were fitted with single exponentials. Mean values ± S.D. of these time constants, derived from four different membrane patches each for controls and 20 μM Pbtx-3, respectively, are shown.

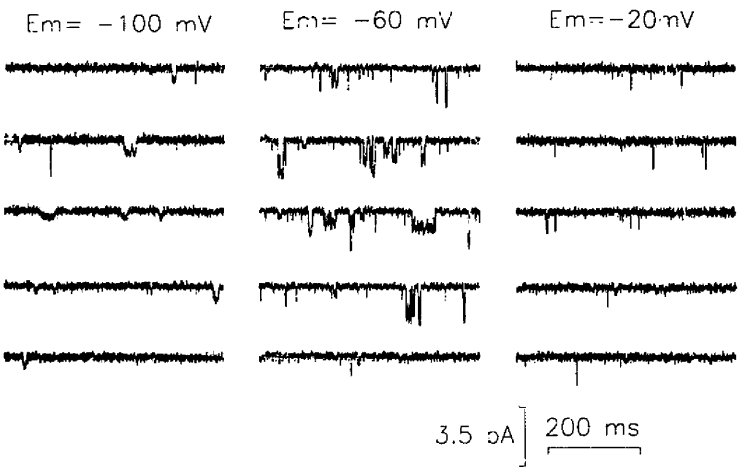

Fig. 2. Openings of sodium channels at constant E_m following administration of 20 μM Pbtx-3. In the absence of Pbtx-3 no such steady-state openings could be detected (not shown). Continuous current traces were replayed from PCM-tape, filtered with a 4-pole Bessel Filter at 3 kHz and digitized at 14 kHz. Segments of such current traces, filtered digitally at 1.5 kHz with a Gaussian filter algorithm are displayed.

practically complete (not shown). Under the influence of 20 μM Pbtx-3, however, openings could be observed even at depolarisations maintained for several minutes, i.e. under steady-state conditions (Fig. 2).

Sodium channel openings observed under steady-state conditions

Sublevel gating under the influence of Pbtx-3 was observed more frequently for sodium channel openings

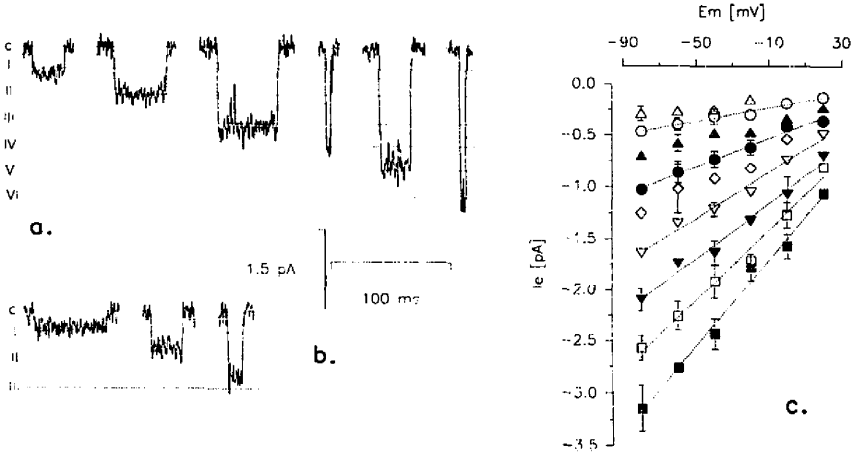

Fig. 3. Subconductance states of Pbtx-3 modified sodium channels at constant E_m. (a) Selected substate gating events making evident the occurrence of substates I to VI. Current traces were filtered digitally at 1.5 kHz. c: closed channel state, lines I to VI were drawn according to the calculated slope conductances from Table I (E_m = −40 mV). (b) Evidence for substates I/2, II/2 and III/2. Digital filtering at 1.5 kHz. c, I, II and III as in (3a), E_m = −40 mV. (c) Mean current amplitudes ± S.D. of substate currents derived from four different cell-attached membrane patches in the presence of 20 μM Pbtx-3, measured from current records filtered digitally at 1.5 kHz. △, I/2; ○, I; ▲, II/2; ●, II; ◇, III/2; ▽, III; ▼, IV; □, V; ■, VI. Dotted lines were drawn according to calculated slope conductances and reversal potentials from Table I for states I, II, III, IV, V and VI, respectively.

at steady state, particularily at negativ. E_m values (Fig. 2, left and middle traces). Sublevel gating of the cardiac sodium channel, induced by mixtures of different gating modifiers has been described previously (Schreibmayer et al. [5]). As described here, Pbtx-3 is unique among gating modifiers of voltage-dependent sodium channels known so far: it is the only modifying agent with which a whole set of subconductance gating events can be induced. In light of this it was of great interest to examine whether this set of events matches the same sublevel pattern as described previously.

Assessment of slope conductances. Steady-state recordings lasting from one minute up to five minutes were recorded at different E_m values. Single-event current amplitudes (I_c's) were measured for a given E_m and found to cluster considerably around distinct levels. Based on this clustering, measured I_c's were grouped into a set of nine classes. For each class one representative single opening event was selected and plotted in Figs. 3a and 3b (E_m: −40 mV). Mean values and standard deviations were calculated and were plotted in Fig. 3c. Slope conductances of sublevel gating events identified in such a way were calculated for E_m values between −80 and +20 mV (in this range I_c vs. E_m was reasonably linear; dotted lines in Fig. 3c, see Table I for summary of results).

Classification of single-event currents based on variance analysis. In order to objectivly classify the I_c's a continuous single-channel trace at a constant E_m of −50 mV was recorded for 57 min. I_c's were assessed by variance analysis as described under Methods and subsequent threshold analysis. It can be seen that I_c's detected in this way cluster around certain current values (Fig. 4) as described above. The given histogram was best fitted by means of a least-square fit with the sum of eight Gaussian functions.

Voltage dependence of sublevel gating. The most interesting feature of Pbtx-3-induced sublevel gating at maintained E_m values was its striking voltage dependence: Whereas at negative E_m values sodium channels opened almost exclusively to substates with low conductivity (Fig. 2, left), at intermediate E_m values almost all the different I_c amplitudes coexisted side by side (Fig. 2, middle) and at more positive E_m values the larger I_c amplitudes dominated (Fig. 2, right). In order to make subsequent analysis of this phenomenon feasible, sublevel current amplitudes were divided into two classes: 'small' sublevels with an I_c amplitude smaller than or equal to level III from Table I and 'large' sublevels with higher I_c amplitudes. 'On'- rates of channel openings were measured for these two sublevel classes and are shown for one particular membrane patch in Fig. 5a. This kind of analysis was performed on four different membrane patches. The

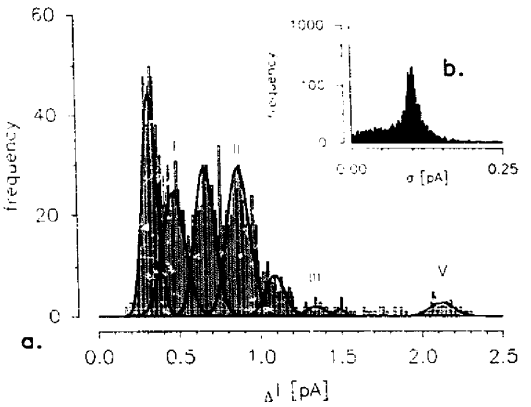

Fig. 4. Jump height analysis of substate currents by means of variance analysis. The patch current of a cell-attached membrane patch, held at E_m −50 mV for 57 min was filtered with a 4-pole Bessel filter at 2 kHz, digitized at 5 kHz and subsequently filtered with a Gaussian filter algorithm at 1 kHz. S.D. of the closed channel current ($\sigma_{I(c)}$) was determined to be 0.146 pA by fitting a simple Gaussian distribution through an amplitude histogram, derived from a segment of the record that did not contain channel openings. Variance analysis as described under Methods was performed. The $\sigma_{I(c)}$ value was set as the variance limit and the minimal window size to 3 ms. Mean I_c and corresponding S.D. (σ) were calculated for each current level detected by simple threshold analysis only from datapoints of the given level fulfilling the variance criterion. The distribution of calculated σ values of individual I_c values as shown in Fig. 4b was not symmetrical, the 'smear' to higher σ values presumably resulting from occasional overlap of channel openings and/or incomplete exclusion of transition currents from the calculation, respectively. The smear to lower σ values presumably is the result of too few datapoints included into the calcuation of I_c and corresponding σ. Therefore jump heights were only calculated for state transitions when $0.092\ pA < \sigma < 0.116\ pA$ for both $I_{c(n)}$ and $I_{c(n+1)}$, when $I_{c(n)}$ is the current level of the state before and $I_{c(n+1)}$ after the transition, respectively. The distribution of the jump heights (dI), calculated as $|I_{c(n+1)} - I_{c(n)}|$ from the remaining 2561 level transitions, is shown in (a) and could be best fitted by the sum of 8 Gaussian functions (solid lines). Although level VI could be detected by eye in the given record at least five times, none of these I_c levels fulfilled the criteria cited above – therefore level VI was lost in this particular case.

TABLE I

Conductance of observed substate openings

Sublevel	Slope conductance ± S.D. (pS)	E_{rev} ± S.D. (mV)
1/2	2.2 ± 0.7	+59 ± 40
I	3.3 ± 0.2	+61 ± 8
II/2	4.4 ± 0.1	+76 ± 5
II	6.9 ± 0.4	+68 ± 6
III/2	8.1 ± 0.9	+71 ± 14
III	11.0 ± 0.7	+68 ± 7
IV	13.3 ± 0.8	+77 ± 8
V	17.1 ± 1.0	+73 ± 7
VI	21.0 ± 1.1	+72 ± 6

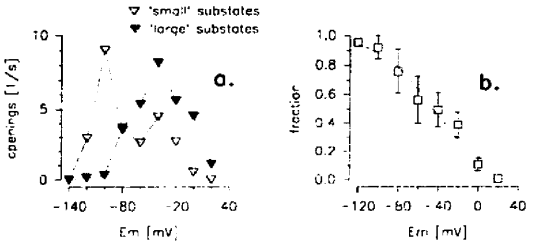

Fig. 5. Voltage dependence of substate gating. Detected channel openings were grouped into two populations: 'small' substates with a corresponding I_c amplitude $\leq E_m \cdot g_{III}$ and 'large' substates with I_c amplitudes $> E_m \cdot g_{III}$. (a) 'On' -rates for openings to 'small' and 'large' substates were measured at different E_m values for one particular patch (records lasted between 44 s and 153 s, respectively). ▽, 'small' substates; ▼, 'large' substates. (b) Fraction of openings to 'small' sublevels detected from the total number of openings. Means ± S.D. from four different membrane patches.

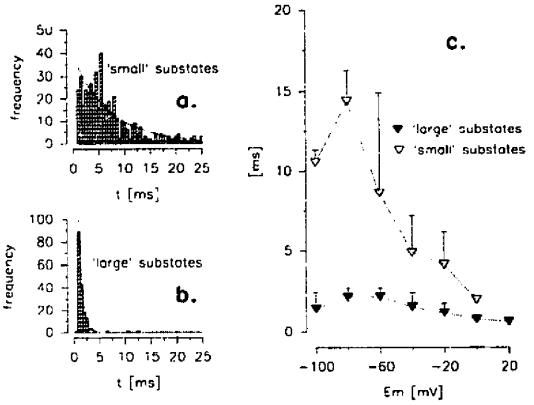

Fig. 6. Microscopic inactivation of substate events. Classification into 'small' and 'large' substates as in Fig. 5. (a) Open time distribution for 'small' substates recorded at a constant E_m of −40 mV. (b) Open time distribution for 'large' substates, same record as for (a). (c) Calculated mean open times for 'small' (▽) and 'large' (▼) substates at different E_m values. Means ± S.D. from four different membrane patches.

contribution of observed openings to 'small' sublevels to the total number of channel openings was calculated for each individual E_m and experiment. The mean

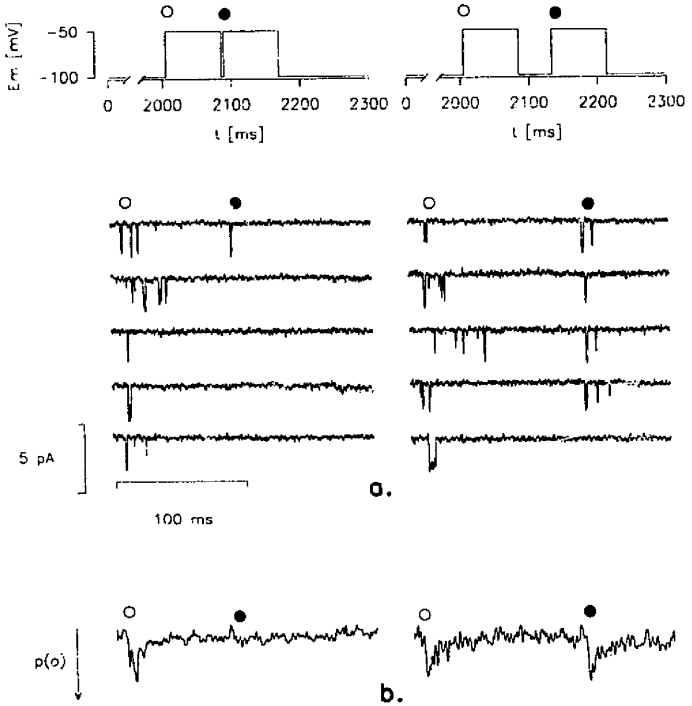

Fig. 7. Analysis of recovery from inactivation at the single-channel level. (a) Double-pulse protocol for the analysis of recovery from inactivation. The patch potential was first kept constant at −100 mV for 2 s, then the first suprathreshold pulse to −50 mV with a duration of 80 ms was applied. Following the recovery time interval at −100 mV (4 ms for left panel and 48 ms for right panel, respectively), a second suprathreshold pulse with 80 ms duration to −50 mV was applied. Open and filled circles indicate the beginning of the first and second suprathreshold pulse, respectively. This protocol was repeated every 2.3 s. Patch currents were filtered with a 4-pole Bessel filter at 2 kHz and digitized at 10 kHz. After filtering at 1.5 kHz with a digital Gauss algorithm, records with no channel openings were averaged and subtracted from each individual record for digital compensation of the capacitance transient. Representative resulting single-channel currents are shown at the bottom of (a). (b) Average currents; downward deflection means increase in $P_{(o)}$, each calculated from 160 consecutive single-channel records corresponding to (a).

values of this fraction at different E_m values are shown in Fig. 5b.

Open dwell times of substates observed under steady-state conditions. Sodium channel substates induced by Pbtx-3 differed not only in their I_c's but also in their open time durations: channel openings to smaller I_c amplitudes were generally of longer duration than those to larger ones (see Fig. 2, middle). In order to quantitate this phenomenon, observed channel openings were divided into two classes based on their individual I_c amplitudes as above. Open times were measured for these different populations and their distribution fitted with a single-exponential function in order to get a measure for their average lifetimes, regardless of the multistate nature of these distribution (see Figs. 6a and 6b for examples of substate open time distribution). These time constants for substate open times were evaluated at different E_m values for four different membrane patches. Their calculated mean values and standard deviations are shown in Fig. 6c.

Recovery from inactivation

The close correlation of substate I_c amplitude with E_m suggested that sublevel gating is closely linked to the activation process. Alternatively, partial recovery from inactivation, especially at maintained depolarisation, might also have accounted for the observed sublevel gating pattern. In order to decide whether stochastic partial recovery occurred, the recovery process of Pbtx-3 modified channels was investigated in detail.

This was accomplished by means of a double pulse protocol as shown in Fig. 7a (top). Following a recovery time interval (dt) of 4 ms at −100 mV sodium channel openings at the beginning of the second suprathreshold pulse could only rarely be observed (Fig. 7a, traces to

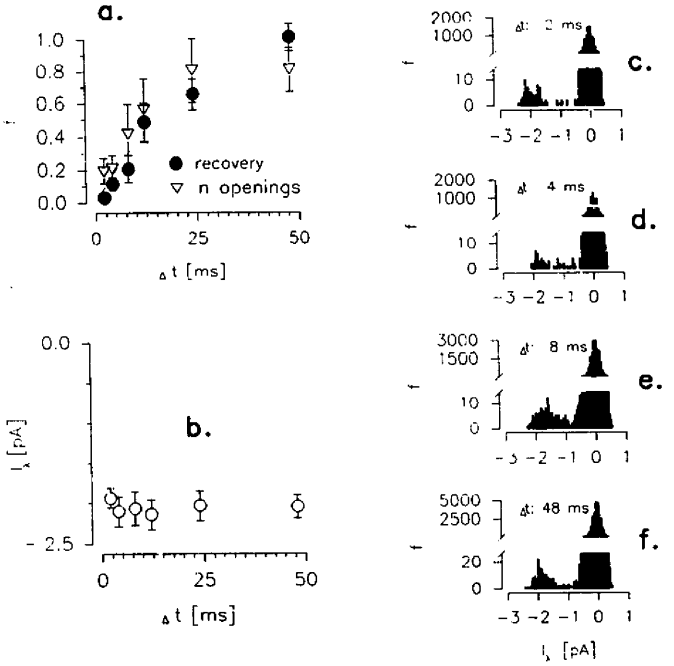

Fig. 8. Contribution of the number of observed channel openings and I_c to the recovery process. (a) ●, Mean values ± S.D. of recovery from inactivation, measured as stated in Results, derived from five different membrane patches in the presence of 20 μM Pbtx-3. The dotted line was drawn according to a simple exponential fit through the data. ▽, Contribution of number of sodium channel openings to the recovery process, expressed as n_2/n_1, when n_2 stands for the number of channel openings detected during the second suprathreshold pulse and n_1 for the number of openings detected during the first pulse, respectively. Mean ± S.D. values. Total counted n_1 values were 1712, 547, 1029, 762 and 1274 and the average n_1's values per pulse were 4.28, 0.98, 2.17, 1.36 and 2.65 for the five different experiments. (b) Mean I_c amplitudes ± S.D. during the second suprathreshold pulse as a function of recovery time interval from the same five experiments. Mean I_c amplitudes were assessed by first performing variance analysis on the current traces obtained from the second suprathreshold pulse (minimal size of window: 1 ms; variance criterion was $\sigma_{(c)}$). Subsequently amplitude histograms were performed from the remaining data points (representative examples are shown in panels c–f) and a simple Gaussian function was fitted through the open-channel current peak, resulting in the average I_c for a given experiment and recovery time interval, respectively.

the left). Accordingly $P_{(o)}$ was low, if not completely negligible (Fig. 7b, left). Recovery approached unity at dt values of 48 ms and above (Figs. 7a and b, right), when measured as $P_{(o)max2}/P_{(o)max1}$, were $P_{(o)max2}$ stands for peak $P_{(o)}$ during the second suprathreshold voltage pulse and $P_{(o)max1}$ for $P_{(o)}$ during the first, respectively (Fig. 8a; filled circles). In one experiment (not shown) recovery from inactivation was also measured for sodium channels in the absence of Pbtx-3. The observations were essentially the same as described here for toxin modified channels. The contribution of both (i) the number of channel openings during a suprathreshold voltage pulse and (ii) the I_e amplitude to the recovery process was analysed. The number of channel openings during the second suprathreshold pulse vs. dt closely matched the time course of the recovery process (Fig. 8a, open triangles). I_e amplitudes were analysed by means of variance analysis (see legend to Fig. 8) and it turned out that I_e amplitudes remained virtually unchanged during the recovery process (see Figs. 8c–f for amplitude histograms and Fig. 8b for mean I_e amplitudes derived from five different membrane patches).

Thus, the recovery process is mainly dominated by the number of sodium channels available, all with similar I_e amplitudes.

Discussion

The present study was designed to explore the functional properties of Pbtx-3 action on single sodium channels from cardiac muscle. A kinetic model for gating conformations of this channel was compiled (Fig. 9) that includes several distinct open states of the channel, each of which represents a conducting conformation of the protein where not all activation gates are open simultaneously.

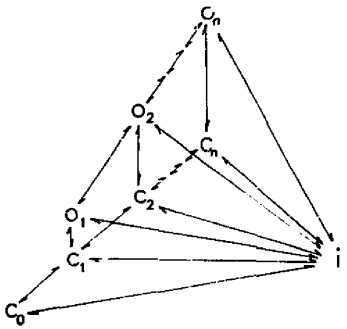

Fig. 9. Proposed scheme for gating of Pbtx-3 modified cardiac sodium channels. Pbtx-3 stabilizes at least nine preopen (c_1 to c_n) and the corresponding open states (o_1 to o_n) thereby promoting channel activation. Rate constants for preopen state interconversions are larger than for channel opening to the corresponding conducting substates. Therefore full channel openings (state designated o_n) dominate immediately after voltage jumps. At maintained depolarization sodium channels open to conducting substates (o_1 to o_n) directly from the inactivated channel state (i), thereby reflecting the conformational state of the channel's activation gates.

Classification of different open states by amplitudes

Substates of the open state with smaller current amplitudes than the maximal possible one have been reported for the major isoforms of sodium channels, i.e. for those from neuronal cells (Nagy [3]), skeletal muscle (Patlak [4]) and cardiac muscle (Schreibmayer et al. [5]). Detection of substates of voltage dependend sodium channels is severely hampered by the low conductance and fast gating of this type of channel. Accordingly, direct evidence of open substates of the cardiac subtype has been possible so far only by using mixtures of different gating modifiers (Schreibmayer et al. [5]). In this sense Pbtx-3 appears to be a gating modifier with unique properties, as it apparently did not stabilize a single, distinct open state. Instead it stabilized a whole set of at least nine different open states as judged from their conductance values. Smaller conductivities of sodium channel substates were certainly not artificially detected, due to bandwith limitations of our recording system as: (i) substate conductance and substate open times were inversely correlated (Fig. 6) and in addition (ii) variance analysis was used for substate detection (Fig. 4). Remarkably, six of these substates (termed here I to VI) fitted fairly well into the pattern observed previously for mixtures of different modifiers. The stabilization of these substates with Pbtx-3 provides additional support for the idea that this substate pattern is an intrinsic property of cardiac sodium channels, not of the gating modifier used. Three additional substates with conductances intermediate to the previously described states could be detected, termed here I/2, II/2 and III/2. The estimated reversal potentials show that Na^+ is the major conducting ion for all observed open states. In view of this observed multiplicity of open substates, it was of great interest to test whether the cardiac sodium channel can assume these substates by (i) switching to open substates with discrete, different conductivities or (ii) randomly locking in certain conductivities out of a continuum of possible conductance values. Specially adapted variance analysis revealed that indeed clustering of I_e values around the assigned substates occurs, indicating (i) as the appropriate hypothesis.

Kinetics of Pbtx-3 modified sodium channels

Effect on sodium channel activation. Although steady-state activation of averaged single-channel currents is shifted considerably to negative potentials, the macroscopic time course for activation (t_a), as well as for the current decay (t_i), were not affected to a greater extent by the action of the toxin. Using *Tityus*

serrulatus (Ts-γ) and *Centruroides noxius* (Cn II-10) toxins as gating modifiers, Yatani et al. [14] observed a similar shift in steady-state activation, albeit accompanied by a marked prolongation of t_a (as termed here). In terms of the modulated receptor hypothesis (MRH, Hondeghem and Katzung [15]) such behavior would be the reflection of high apparent affinities of preopen states (termed c_1 to c_n in the scheme in Fig. 9), but not of the corresponding open states to these modifiers. Shift of steady-state activation without affecting the activation time course as observed in our case would, in terms of the MRH, mean similar high affinities to preopen states c_1 to c_n and to the corresponding open states. Of course similar conclusions would be reached also in terms of the guarded receptor hypothesis (Starmer et al. [16]).

Microscopic inactivation of channel openings immediately after voltage jumps. As the time constant for channel open times (t_o) is much smaller than that observed for macroscopic current decay (t_i) in most cases, t_i is most likely dominated mainly by the time course of activation of sodium channels. This was confirmed in our case for E_m: −40 mV as t_o increased about 2-fold, when compared to controls, but t_i was apparently not affected. Thus at this potential, unchanged t_i is most likely a reflection of unchanged t_a. Another interesting observation was that the effect of Pbtx-3 on t_o of the fully conducting open state was only minor compared to other gating modifiers that inhibit inactivation, e.g. veratridine (Sigel [2]).

Kinetics of sodium channel openings at maintained depolarisation. Two types of sodium channel openings at maintained depolarisation have already been observed for cardiac (Patlak and Ortiz [17]) as well as for skeletal (Patlak and Ortiz [18]) muscle sodium channels: single openings that account for most of these 'late' channel openings and openings occurring occasionally in long bursts. Whereas the latter have been attributed to be the result of occasional failure of the inactivation gate unmasking in this way frequent interconversions between the rested and open channel states, the former have been attributed to result from sodium channels that return directly from the inactivated state to the open channel state. Whereas the voltage range were such steady-state openings can be observed is rather limited under physiological conditions, this can be greatly extended with the aid of Pbtx-3, which stabilizes preopen and open channel states as well. The idea that steady-state openings of Pbtx-3-modified channels result from channel openings from the inactivated channel state is strongly supported by the observation that many of these channel openings differ in their I_c amplitude and their inactivation kinetics from those observed in most cases at the beginning of a voltage pulse (representing channel openings from closed states).

Furthermore both t_o and I_c amplitudes were dependent on E_m. This indicates that Pbtx-3 interferes with the channel's activation gates not only via a shift of steady-state activation, but also by induction of specific substates, depending on the conformational state of these gates, which, in turn, depends on E_m. In other words, the observed increase of g_c amplitude and decrease of t_o with increasing depolarisation are most likely reflections of the channel's quantal activation process (Hodgkin and Huxley [19]). Given the case that the rate constant for the rested-inactivated transition is smaller than for the open-inactivated one, prolongation of t_o, as observed in our case, is directly predicted from the theory of allosteric processes (Monod et al. [20]) when not all of the activation gates are in the 'active' conformation.

The conclusion that each nonconducting preopen state might be accompanied by a corresponding subconductance state, raises the question, what might be the physical correlate to this complicated behaviour? Molecular cloning techniques in connection with electrophysiology on mutated and expressed ion channels have revealed that sodium channel activation gates are most likely identical with a unique structural motif, the so-called S4 helix of voltage-dependend ion channels (Stuehmer et al. [21]). The existence of conducting and nonconducting conformations for each possible physical state of the gates would imply that voltage-dependent conformational activation of these S4 helices is not identical with, but merely the precursor of channel opening, which itself is probably accompanied by major changes in α-subunit conformation. Open substates could be the manifestation of partial activation only of several coexisting pathways for sodium ions within one channel entity, whatever their structural basis may be (Schreibmayer et al. [5]).

Comparison of Pbtx-3 with other gating modifiers

Based on their characteristic functional interaction with single sodium channels, gating modifiers can be grouped into several distinct classes:

(i) Modifiers that interact with and block the open state of sodium channels like TTX and STX (Dugas et al. [22]).

(ii) Agents like veratridine, germitrine, batrachotoxin etc. that bind to and stabilize the open sodium channel (Quandt and Narahashi [1] and Sigel [2]). Inactivation is greatly delayed by these substances but complete, when once occurred. Under the influence of such a modifier, open sodium channels often switch to open substates with lower conductivity (Schreibmayer et al. [5]).

(iii) Other modifiers like sea anemone toxins and α-scorpion toxin also stabilize open states, but mainly act on the inactivation gate, shifting its voltage dependence considerably to more positive potentials. As a

result channels frequently open in bursts at maintained depolarisation (Schreibmayer et al. [12] and Kirsch et al. [23]).

Modifiers of type (ii) and (iii) interact allosterically (Catterall [24]), as sodium channels under the action of type (iii) agents open frequently even at maintained depolarization and thereby provide the binding sites for modifiers of type (ii) (Schreibmayer et al. [5], Wang et al. [25] and O'Leary and Krueger [26]). Because of their peculiar behaviour, which leads to prolonged or increased numbers of channel openings, modifiers of types (ii) and (iii) are often referred to as the so called 'channel openers'. From the more mechanistic studies on the molecular level cited above, however, it becomes clear that these agents merely act via stabilization of already open channels (ii) or reactivation of inactivated channels (iii), than by directly promoting the activation process. Instead the term 'channel' openers should be reserved for modifiers of type (v) as described below.

(iv) Cn II-10 and *Tityus serrulatus* γ toxin have been reported to shift steady-state activation to more negative potentials, accompanied by a marked delay in sodium current activation, probably by interacting with and stabilizing preopen states of the sodium channel (Yatani et al. [14]).

(v) In the present study a gating modifier was examinated that also acts on preopen sodium channel states, but does not stabilize them at the cost of open states. Instead a whole set of different open states is uncovered that is obscured by fast preopen, but nonconducting, state interconversions under physiological conditions.

Acknowledgements

The authors would like to thank L. Hymel (New Orleans) for his helpful comments on the manuscript. The inspiring interactions and discussions with our colleagues N. Dascal (Tel Aviv), H. Glossmann (Innsbruck), D. Platzer (Graz), H. Schindler (Linz), O. Tripathi (Lucknow) and H.A. Tritthart (Graz) are gratefully acknowledged. We thank B. Spreitzer for excellent myocyte preparations and A. Russ for programming our computers. This work was made possible by a grant from the Austrian Research Foundation (S4504B).

References

1 Quandt, F.N. and Narahashi, T. (1982) Proc. Natl. Acad. Sci. USA 79, 6732–6736.
2 Sigel, E. (1987) Pfluegers Arch. 410, 112–120.
3 Nagy, K. (1987) Eur. Biophys. J. 15, 129–132.
4 Patlak, J.B. (1988) J. Gen. Physiol. 92, 413–430.
5 Schreibmayer, W., Tritthart, H.A. and Schindler, H. (1989) Biochim. Biophys. Acta 986, 172–186.
6 Baden, D.G. (1989) FASEB J. 3, 1807–1817.
7 Borison, H.L., McCarthy, L.E. and Ellis, S. (1985) Toxicon 23, 517–524.
8 Lombet, A., Bidard, J.N. and Lazdunski, M. (1987) FEBS Lett. 219, 355–359.
9 Sharkey, R.G., Jover, E., Couraud, F., Baden, D.G. and Catterall, W.A. (1987) Mol. Pharmacol. 31, 273–278.
10 Gusovsky, F., Rossignol, D.P., McNeal, E.T. and Daly, J.W. (1988) Proc. Natl. Acad. Sci. USA 85, 1272–1276.
11 Schreibmayer, W., Tritthart, H.A., Zernig, G. and Piper, H.M. (1985) Eur. Biophys. J. 11, 259–263.
12 Schreibmayer, W., Kazerani, H. and Tritthart, H.A. (1987) Biochim. Biophys. Acta 901, 273–282.
13 Hamill, O.P., Marty, A., Neher, E., Sakman, B. and Sigworth, F.J. (1981) Pfluegers Arch. 391, 85–100.
14 Yatani, A., Kirsch, G.E., Possani, L.D. and Brown, A.M. (1988) Am. J. Physiol. 254, H443–H451.
15 Hondeghem, L.M. and Katzung, B.G. (1977) Biochim. Biophys. Acta 472, 373–398.
16 Starmer, C.F., Grant, A.O. and Strauss, H.C. (1984) Biophys. J. 46, 15–27.
17 Patlak, J.B. and Ortiz, M. (1985) J. Gen. Physiol. 86, 89–104.
18 Patlak, J.B. and Ortiz, M. (1986) J. Gen. Physiol. 87, 305–326.
19 Hodgkin, A.L. and Huxley, A.F. (1952) J. Physiol. Lond. 117, 500–544.
20 Monod, J., Wyman, J. and Changeux, J. (1965) J. Mol. Biol. 12, 88–118.
21 Stuehmer, W., Conti, F., Suzuki, H., Wang, X., Noda, M., Yahagi, N, Kubo, H. and Numa, S. (1989) Nature 339, 597–603.
22 Dugas, M., Honerjaeger, P. and Masslich, U. (1989) J. Physiol. Lond. 411, 611–626.
23 Kirsch, G.E., Skattebol, A., Possani, L.D. and Brown, A.M. (1989) J. Gen. Phyiol. 93, 67–83.
24 Catterall, W.A. (1975) Proc. Natl. Acad. Sci. USA 72, 1782–86.
25 Wang, G., Dugas, M., Armah, B.I. and Honerjaeger, P. (1990) Mol. Pharmacol. 37, 144–48.
26 O'Leary, M.E. and Krueger, B.K. (1989) Mol. Pharmacol. 36, 789–795.